

LARGE-SCALE COMPUTATION OF TRANSIENT ELECTROMAGNETIC FIELDS REGARDING THE FIELD QUALITY IN THE APERTURE OF THE SIS100 DIPOLE MAGNET*

Stephan Koch[§], Thomas Weiland, TEMF, TU Darmstadt, Darmstadt, Germany

Abstract

For the computation of the electromagnetic fields in large accelerator components, such as the superconducting dipole magnets to be installed in the heavy-ion synchrotron SIS100 at GSI, Darmstadt in context of the FAIR project, very large numerical models are required. By using parallelization techniques in combination with higher-order finite element approaches, full 3D solutions for the complicated geometry can be obtained in reasonable computational time. A parallelized 3D simulation tool is developed and applied to determine the field quality of a prototype of the SIS100 dipole magnet. The results for the field quality during transient operation considering eddy currents in the conductive parts of the assembly are reported.

INTRODUCTION

The design of the SIS100 dipole is based on the Nuclotron geometry [1]. Several modifications aiming at the improvement of the field quality as well as at the reduction of the eddy-current losses during transient operating conditions have been proposed [2, 3]. In the early phase of the design process, commonly 2D simulations considering only the cross-section of the dipole yoke are performed in order to optimize the field quality in the aperture [3]. Furthermore, dynamic effects, e.g., resulting from eddy currents in conductive parts of the yoke assembly are neglected in this stage. Here, transient 3D simulations considering the formerly neglected effects are carried out. Results for the field quality are reported in terms of relative circular multipole coefficients for the aperture field. The yoke geometry shown in Fig. 1(a) is taken from a full-length ($\ell = 2.8$ m) prototype of the SIS100 dipole already delivered to GSI, Darmstadt. Above as well as below the two-layer coils, air slits and a negative shimming are applied in order to enhance the field quality in the rectangular aperture (Fig. 1(b)) the dimensions of which are $182 \text{ mm} \times 68 \text{ mm}$. During the expected operating conditions, a ramp rate of 4 T/s up to the maximum aperture flux density of 1.9 T to 2.1 T is required. As a consequence, eddy-currents arise especially in the end regions of the laminated yoke as well as in the conductive beam pipe. These electric losses lead to an undesired heating of the respective model parts and, at the same time, cause a deterioration of the dipole field in the aperture. In particular the effect of the eddy currents

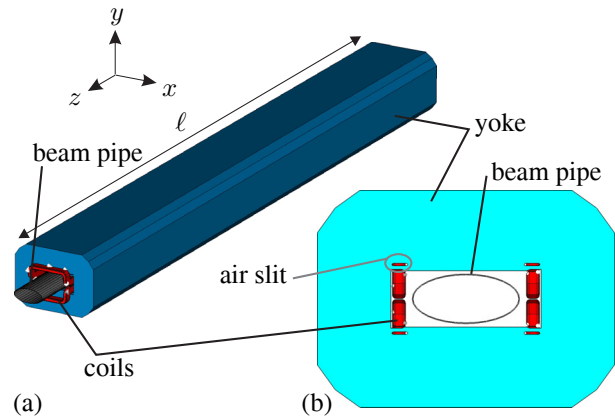


Figure 1: Geometry of the full-size prototype dipole magnet (length $\ell = 2.8$ m) considered in the numerical simulations: (a) 3D view of the yoke and the superconducting coil pair including an elliptical beam pipe (major and minor half-axes 65 mm and 30 mm, respectively); (b) 2D view of the yoke cross-section.

close to the end regions of the yoke can only be calculated using transient 3D simulation techniques. Due to the yoke length of $\ell = 2.8$ m, a very large number of numerical degrees of freedom is required in order to resolve the relevant geometrical details by means of a volume discretization approach.

TRANSIENT FIELD FORMULATION

For the effects under consideration here, capacitive phenomena can be neglected. Under this assumption, introducing the magnetic vector potential \mathbf{A} according to

$$\mathbf{B} = \nabla \times \mathbf{A}, \quad (1)$$

with \mathbf{B} the magnetic flux density, leads to the magnetoquasistatic formulation

$$\nabla \times (\nu(\mathbf{B}) \nabla \times \mathbf{A}) + \sigma \frac{\partial}{\partial t} \mathbf{A} = \mathbf{J} \quad (2)$$

of the Maxwell equations in the time domain. Here, $\nu = 1/\mu$ denotes the tensor-valued nonlinear reluctivity, σ the electric conductivity tensor and \mathbf{J} the source current density.

The formulation in Eq. 2 is discretized in space by means of finite element (FE) shape functions of selected order on a tetrahedral mesh. For temporal discretization, the backward Euler method using a constant time step Δt is applied. In order to take the yoke lamination into account, a

* Work supported by GSI Helmholtzzentrum für Schwerionenforschung GmbH, Darmstadt under contract F&E, DA-WE11

[§] koch@temf.tu-darmstadt.de

homogenization strategy based on the packing factor γ_p , as described in [4], resulting in anisotropic local material coefficients ν and σ is used. Therefore, a nonlinear algebraic system of equations has to be solved. The nonlinearity corresponding to the ferromagnetic saturation of the iron yoke is resolved by means of a Newton-Raphson scheme applied within each time step Δt .

FIELD QUALITY

As the aperture region of the dipole magnet is homogeneous as well as source-free, the magnetic flux density \mathbf{B} is both irrotational and divergence-free. Therefore, the related field distribution is a solution of Laplace's equation in terms of a scalar potential V or, alternatively, a vector potential \mathbf{A} . In the following, only the 2D case in terms of cartesian coordinates with z aligned to the beam axis is considered. The multipole expansion of the transversal flux density under the essential condition $B_z = 0$ is given by

$$B(\underline{z}) = B_y + iB_x = \sum_{n=1}^{\infty} \underline{C}_n \left(\frac{z}{R}\right)^{n-1} \quad (3)$$

with the complex quantity $\underline{z} = x + iy$ and a reference radius R [5]. Given a consistent numerical field solution $B_x(x, y)$ and $B_y(x, y)$ at a circle $r = \sqrt{x^2 + y^2}$ the harmonic expansion coefficients \underline{C}_n are obtained using a discrete Fourier transformation (DFT). The normal and skew multipole coefficients B_n and A_n are defined as

$$\begin{aligned} B_n &= \Re\{\underline{C}_n\} \\ A_n &= \Im\{\underline{C}_n\}. \end{aligned} \quad (4)$$

Typically, the field quality is specified relative to the dominating harmonic coefficient which is, in this case, the normal dipole B_1 .

However, the field distribution obtained from 3D simulations in general exhibit a non-vanishing z -component of the magnetic flux density. Therefore, two different strategies in order to perform an analysis of the transversal field quality in terms of multipoles are considered:

1. Evaluate the magnetic flux density only at the center of the magnet ($z = 0$ in Fig. 2), where $B_z = 0$ is explicitly enforced by means of an appropriate symmetry constraint on the fields during the numerical simulation. 3D effects, e.g., due to eddy-currents and local saturation in the end regions, are, therefore, neglected.
2. Sample the calculated 3D field at numerous circles along the magnet axis (z) and use the integral field

$$\mathbf{B}^{\text{int}}(x, y) = \int_{-\infty}^{+\infty} \mathbf{B}(x, y, z) dz \quad (5)$$

for the multipole expansion. For the actual determination of the integral field, however, the integration range is limited to the interval $[-z_{\text{max}}; z_{\text{max}}]$ in Fig. 2 where the actual values of \mathbf{B} already decayed sufficiently.

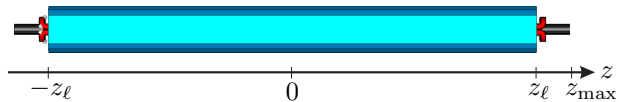


Figure 2: Longitudinal view of the magnet model indicating the positioning along the z -axis with $z_l = \ell/2 = 1.4$ m.

Table 1: Comparison of the relative integral multipole coefficients (in units, 10^{-4}) based on the center field (quasi-2D) as well as on the 3D field solution (3D). Two configurations, with and without beam pipe, of the dipole assembly are considered. Multipole coefficients are listed both for static and transient simulations, whereas in the latter case the maximum values over the excitation cycle are selected.

$r_{\text{ref}} = 28$ mm		static		transient	
		beam pipe no	beam pipe yes	beam pipe no	beam pipe yes
$\frac{B_3^{\text{int}}}{B_1^{\text{int}}} / 10^{-4}$	quasi-2D	3.62	3.56	3.62	3.70
	3D	8.53	8.46	8.49	8.54
$\frac{B_5^{\text{int}}}{B_1^{\text{int}}} / 10^{-4}$	quasi-2D	0.33	0.32	0.33	0.32
	3D	0.78	0.79	0.78	0.79
$\frac{B_7^{\text{int}}}{B_1^{\text{int}}} / 10^{-4}$	quasi-2D	0.13	0.13	0.13	0.13
	3D	0.15	0.15	0.15	0.15

In order to compare the influence of 3D as well as transient effects on the field quality, the integration in Eq. 5 is carried out once assuming the center field $\mathbf{B}^C(x, y, z = 0)$ as constant inside the yoke ($-z_l < z < z_l$) and zero otherwise. Secondly, the calculated values for the different positions on the z -axis are considered for the integration. From the difference in the obtained coefficients the effect of the 3D geometry on the integral field quality can be determined.

NUMERICAL RESULTS

Two configurations of the SIS100 prototype dipole are simulated, one without the and one including the elliptical beam pipe. Its thickness is selected to 1 mm and $\sigma = 10^6$ S/m is chosen for the electrical conductivity in the simulations. The laminated yoke is modeled using a homogenization procedure considering a packing factor of $\gamma_p = 0.995$ in combination with the related nonlinear saturation characteristics. For the transient simulation, ramp 2c from [6] is used. It features an injection phase of 0.4 s at 12% of the maximum current followed by a linear ramping at 4 T/s up to the maximum current in the superconducting coils. A flat-top of 0.1 s provides the extraction phase. Subsequently, a symmetric down-ramping is applied.

The relative integral multipole coefficients calculated according to Eq. 5 at the reference radius $r = 28$ mm are summarized in Table 1. Within the selected limits of the accuracy of the numerical simulation carried out here, no significant changes in the listed values for the relative multipole coefficients $B_n^{\text{int}}/B_1^{\text{int}}$ with $n = 5$ and $n = 7$ are

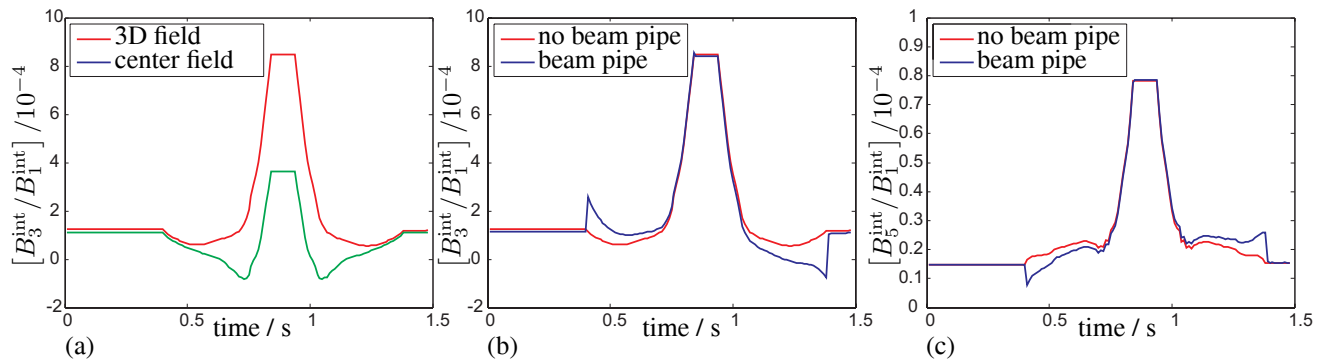


Figure 3: (a) Comparison of the integral sextupole coefficients based on the 3D field solution and on the central field at $z = 0$ for the configuration without beam pipe; (b) Integral sextupole coefficients (3D field) for the different models with and without beam pipe; (c) Integral decapole coefficients (3D field) for the different models with and without beam pipe.

observed when comparing the different simulation scenarios. However, in case of considering the 3D structure of the dipole magnet in terms of integrating the true 3D field distribution over the length in z -direction, the coefficients for $n = 3$ and $n = 5$ increase by approximately a factor of 2. As this behaviour occurs also in the static case, it can be assigned mainly to the geometry of the magnet as opposed to, e.g., eddy-currents near the end regions. These seem to play an inferior role with respect to the reported transient peak values of the coefficients which arise at the flat-top of the excitation cycle as can be seen in Fig. 3(a) for the integral sextupole coefficient. While the relevant relative multipole coefficients are well below the design specification of $6 \cdot 10^{-4}$ when accounting for the center field only, the limit is exceeded as soon as the 3D field distribution is considered. Even though the peak values of the multipole coefficients for the transient simulations considering the conductive beam pipe are almost equal to the ones obtained without the respective model part, the behaviour with respect to the time axis differs, nonetheless. As shown in Fig. 3(b) for the relative sextupole coefficient, a sharp rise occurs at the beginning of the acceleration cycle at $t = 0.4$ s for the configuration including the beam pipe. However, the resulting peak is still well below the maximum allowed value. Furthermore, the almost symmetric shape of the graph with respect to the middle of the flat-top is lost in this case due to the time constants of the eddy-currents in the conductive model parts. A similar observation can be made for the decapole coefficient shown in Fig. 3(c), however, to an even lower extend already below one unit (10^{-4}).

The determination of the field quality based on circular multipoles as described here, however, does not ideally cover the rectangular aperture of the dipole magnet under consideration. In particular at injection field level, the large beam size requires a high field quality over the entire elliptical cross-section of the beam pipe. Therefore, a better characterization of the field inside this specific aperture geometry can be found by using elliptical multipoles as described, e.g., in [7].

CONCLUSION

3D magnetostatic simulations provide a reasonable estimate for the integral multipole coefficients in the full-length prototype of the SIS100 dipole. Additional effects which are not related solely to the geometry of the yoke can be observed in the transient case. However, for the simulations reported in this paper, the magnitude of the dynamic changes in the multipole coefficients is still below the design specification.

REFERENCES

- [1] A. Kovalenko. Status of the Nuclotron. In *Proceedings of the 4th European Particle Accelerator Conference (EPAC94)*, pages 161–164, London, UK, June 1994.
- [2] A. D. Kovalenko, N. N. Agapov, V. G. Aksenov, I. E. Karpunina, H. G. Khodzhbagiyani, G. L. Kuznetsov, M. A. Voevodin, G. Moritz, E. Fischer, G. Hess, and C. Muehle. Progress in the design and study of a superferic dipole magnet for the GSI fast-pulsed synchrotron SIS100. *IEEE Transactions on Applied Superconductivity*, 14(2):321–324, June 2004.
- [3] A. Kalimov, G. Moritz, and A. Zeller. Design of a superferic dipole magnet with high field quality in the aperture. *IEEE Transactions on Applied Superconductivity*, 14(2):271–274, June 2004.
- [4] S. Koch, H. De Gersem, T. Weiland, E. Fischer, and G. Moritz. Transient 3D finite element simulations of the SIS100 magnet considering anisotropic, nonlinear material models for the ferromagnetic yoke. *IEEE Transactions on Applied Superconductivity*, 18(2):1601–1604, June 2008.
- [5] A. K. Jain. Basic theory of magnets. In *CAS - CERN Accelerator School: Measurement and Alignment of Accelerator and Detector Magnets, Anacapri, Italy, 11 - 17 Apr 1997*, pages 1–26, 1998.
- [6] GSI. FAIR Baseline Technical Report. Available online at www.gsi.de, March 2006.
- [7] P. Schnizer, B. Schnizer, P. Akishin, and E. Fischer. Magnetic field analysis for superferic accelerator magnets using elliptical multipoles and its advantages. *IEEE Transactions on Applied Superconductivity*, 18(2):1605–1608, June 2008.